5-11-2016

Independent Study: Microfluidic Channel for Acoustic Particle Manipulation

Stefanie T. Shahan
Washington University

J. Mark Meacham
Washington University in St. Louis

Stefanie Shahan

Independent Study Project

Washington University in St. Louis

Under the Supervision of Dr. J Mark Meacham

Abstract

To study acoustic microfluidic particle manipulation, a microfluidic channel was designed in AutoCAD and fabricated in a silicon wafer using potassium hydroxide etching and other cleanroom techniques. The first channel created was destructively tested and its fabrication techniques characterized; future channel development is outlined.

Introduction

I participated in a research project under the supervision of Dr. J. Mark Meacham in support of a minor in Nanoscale Science from the School of Engineering and Applied Sciences at Washington University in St. Louis. The primary goal of the independent study was the development and testing of an acoustic microfluidic device for targeted manipulation of biological particles in heterogeneous suspensions.

Acoustic separation of particles, known as acoustophoresis, utilizes the inherent differences between the particles and the medium they are in. These geometric and compositional differences, summarized in the acoustic contrast factor (ACF) determine the magnitude of the resulting acoustic radiation force (ARF) and terminal particle location when a heterogeneous mixture is exposed to a standing acoustic wave. If the sign of the ACF is positive (negative), the particles will migrate to the pressure nodes (antinodes) of the field, which are their respective lowest energy states. The induced force is relatively low, allowing acoustophoresis to be used in biomedical applications ranging from cell separation to dialysis or purification.

Dr. J. Mark Meacham has been working with acoustic microfluidics for an extended period of time. His lab has typically implemented a bulk transducer to generate an ultrasonic standing wave within microfluidic channels to manipulate particles and atomize fluid mixtures.

In my supervised independent study, with the help of Professor Meacham and PhD student Michael Binkley, I was able to develop a microfluidic channel in silicon through CAD and cleanroom fabrication, and to optimize the channel geometric parameters within a CAD file for a refined mask. Specifically, I solidified functional fabrication methods for a silicon channel using available facilities at Washington University.

Methods and Results

In the fall semester of 2015, a device was designed, which was inspired primarily by an existing microfluidic particle separator (Augustsson et al., 2012). Augustsson et al. (2012) presented the creation of an acoustophoresis microchannel fabricated in silicon using standard photolithography and anisotropic KOH wet etching. The resulting microchannel consisted of an inlet, a cell pre-alignment channel, a flow splitter, a cell separation channel, and a trifurcation outlet (see *Figure 1*). A piezoceramic transducer and Peltier element were used to generate temperature-regulated acoustophoresis.

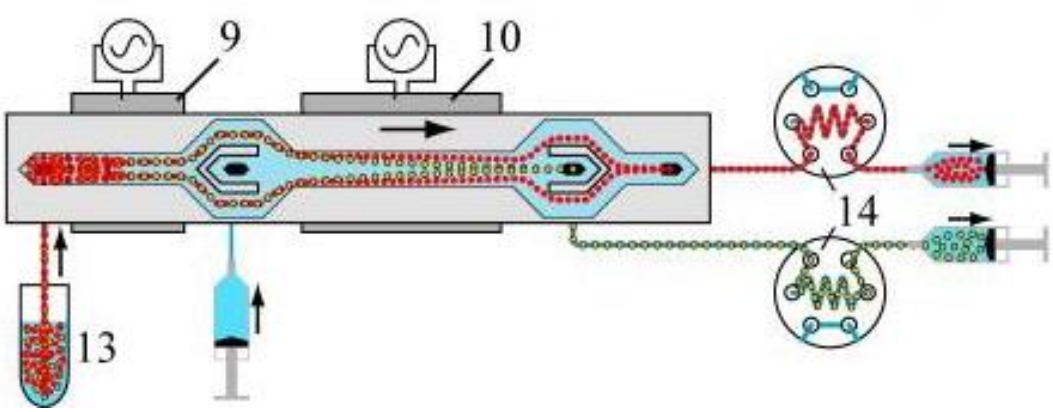

Figure 1. A microchannel for acoustophoresis, designed by Augustsson et al. (2012).

For our purposes, the primary use of such a device is experimental determination of the operating parameters that affect ACF. Control will be run with particles whose properties are known (such as polystyrene beads), and measured parameters will be used to calculate the ACF (and potentially density and compressibility) for particles whose properties are unknown (cells). Naturally, the device would also be capable of separating particles with differing properties.

For this project, microchannels were fabricated in silicon following the steps listed in *Figure 2*. Utilizing the known etch rates of the various crystal planes of silicon and the final channel geometry produced by Augustsson et al. (2012), I designed in AutoCAD a photomask capable of meeting all experimental conditions required for determining the ACF of various cell types and polymeric beads (Mask A).

The design of these channels was based on literature related to KOH etching of silicon. Wet KOH etch rates differ within silicon, depending on crystal plane: {110} has the largest etch rate, followed by etch rate of {100}, and a minimal etch rate of {111}. These differences in etch rates allow the fabrication of specific geometries; an example from literature may be seen in *Figure 3* (Pal et al., 2015).

Mask A shown in *Figure 4* was created with the assumption that etch rate at a 45° angle from the wafer flat was 1.5 times that of the etch into the wafer due to the difference in the rate of {110} and {100} KOH etching—this was later experimentally found to be a one to one ratio as planes at 45° to the wafer flat are {100} as is the plane of the wafer surface.

Mask A included two microchannels (see *Figure 4*) with two bifurcations, an inlet, and an outlet for each channel. These channels differed slightly in their bifurcation “node” geometry as can be seen in *Figure 5a,b,* which allowed differences in etched shapes resulting from the different geometries to be determined.

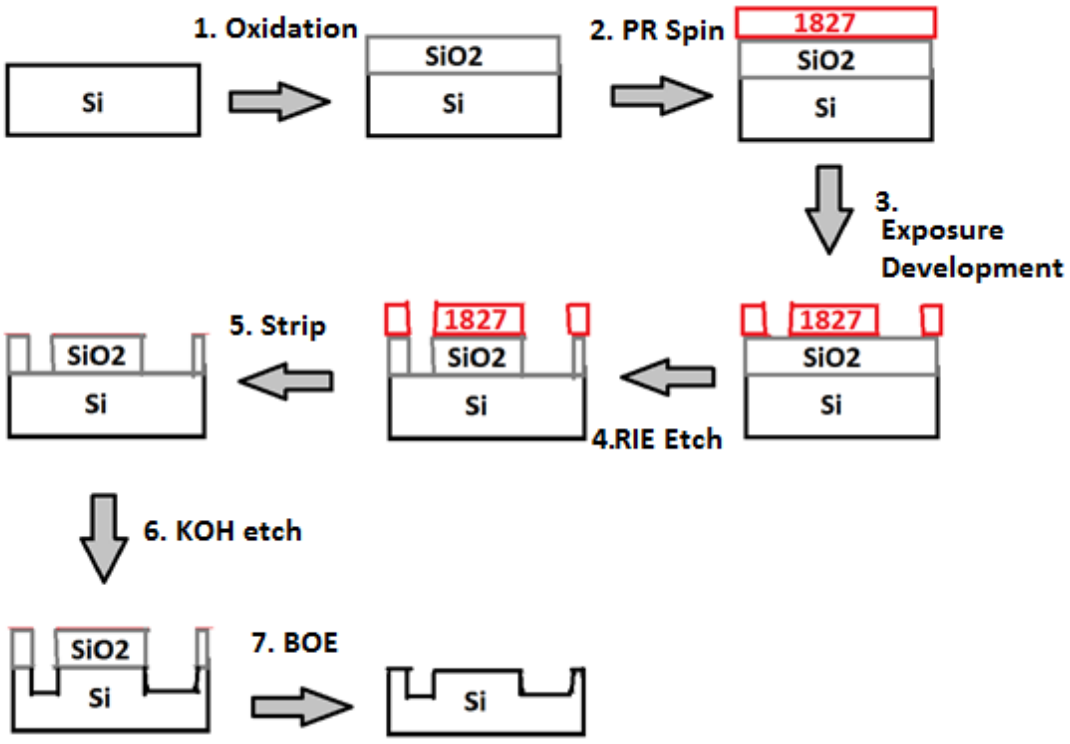

Figure 2. Flow diagram of the processing of the wafer to etch a channel in Si.

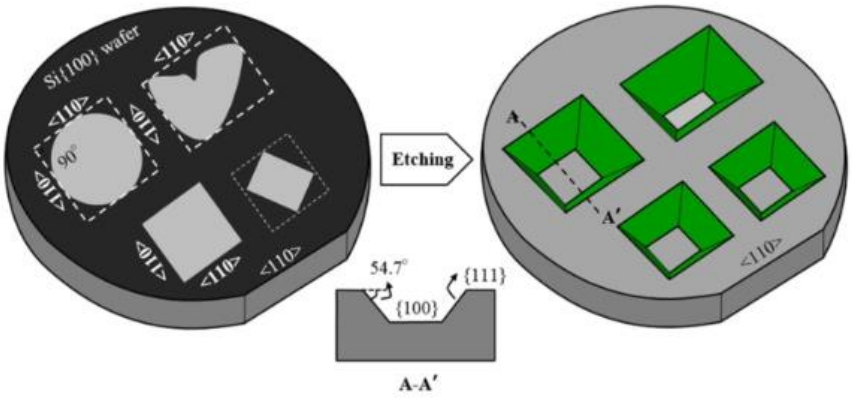

Figure 3. A diagram of the results of a KOH etch on a wafer similar to that used in this study. Lines perpendicular or parallel with the wafer flat <110> are not etched due to low etch rate of the {111} planes, but a line 45° from the wafer flat would allow for etching perpendicular to that line (Pal et al., 2015).

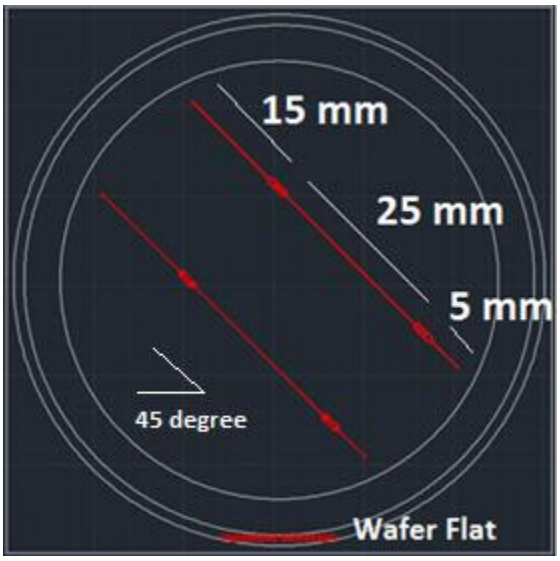

Figure 4. Mask A, the CAD drawing produced as a mask for photolithography of a silicon wafer.

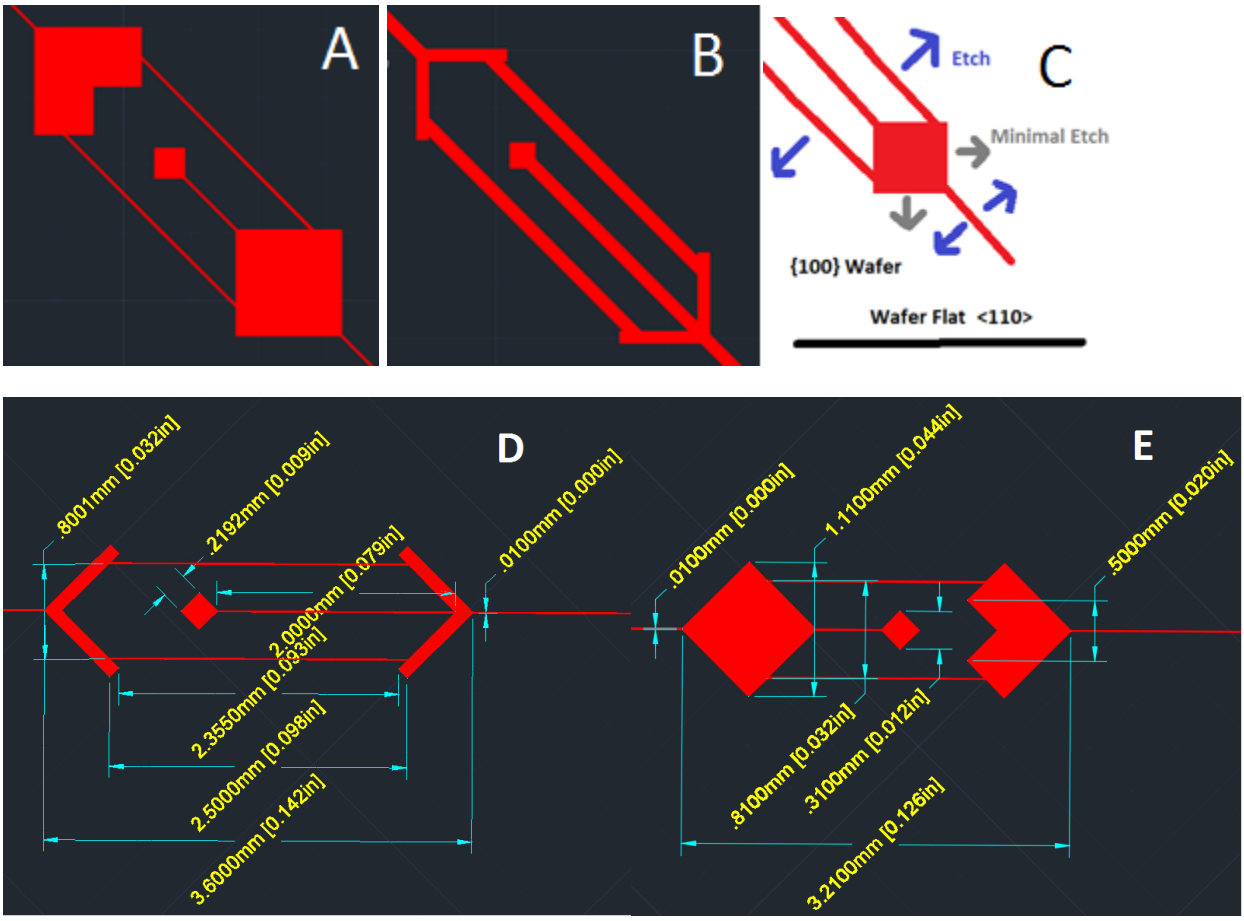

Figure 5a,b. An expanded view of bifurcation node geometry within the CAD drawing of Mask A. 5c. A drawing to exemplify the intended KOH etching for this mask. 5d,e. Same expanded view as in part a, b, including measurements.

A 3 inch silicon {100} wafer was cleaned with a 3:1 mixture of H_2SO_4 with H_2O_2 in solution (Piranha solution) and stripped of SU8 photoresist residue from previous fabrication work. The wafer (referred to henceforth as DW1) was oxidized at 1100°C (*Figure 2, step 1)* for an indeterminate period of time, as the furnace mistakenly ran for an entire weekend. DW1 was oxidized until it reached a thickness of roughly 858.04nm. This thickness was intended to fully protect silicon during a KOH etch of silicon to a depth of 100 µm. Si and SiO_2 are etched at different rates in KOH solution, allowing the production of a designed geometry through reduction of Si surface exposure. It was assumed that the etch ratio in 45% KOH at 60°C is roughly 90 nm silicon dioxide: 20 µm silicon (Madou, 2012).

DW1 was dehydrated for 10 minutes at 200°C before being cooled and exposed to a hexamethyldisilazane (HMDS) primer to prepare it for the positive photoresist SC1827. The SC 1827 was spun using the parameters in *Table 1* (*Figure 2, step 2*), chosen to produce a thickness of roughly 3200 nm, capable of protect unetched areas of silicon dioxide from a reactive ion etch (RIE) of the mask pattern. This thickness was chosen with the assumption that selectivity of SiO_2:resist was roughly 1:4, meaning for every 1 nm of SiO_2 etched 4 nm of photoresist would be etched. It was found that taking photoresist from the middle of the bottle for spinning reduced the presence of impurities in the photoresist layer (there was coagulation on the bottom of the bottle).

Table 1. Parameters for SC1827 photoresist spinning of DW1.

Steps (speed, ramp acceleration, duration of step)
500rpm/100/5s
2000rpm/500/30s
0rpm/500/4s

DW1 was soft baked for 60 seconds at 115°C and then exposed for 18 seconds with alignment of Mask A to the wafer flat using the alignment features at the bottom of the mask (see *Figure 4*). The mask must be aligned to the wafer flat to implement the different etch rates of Si and create the intended geometry (see *Figure 5c* for a visualization of this etching). The importance of this alignment was discussed earlier in detail within the section on Mask A. The wafer was developed in MF 319 for 40 seconds (*Figure 2, step 3*), and profilometry measurements found the photoresist to be at a depth of -33,973 Angstroms, sufficient for protection of the silicon from KOH attack. The primary gas used in the SiO_2 etch was CF_4, resulting in the reaction: $CF_4 + SiO_2 \Rightarrow SiF_4 + O_2$, where SiF_4 and O_2 are gases that are pumped out, leaving the system. DW1 was put through RIE for roughly 24 minutes in total to transfer the mask pattern into the SiO_2 (*Figure 2, step 4)*. DW1 was then stripped of photoresist residue with acetone (*Figure 2, step 5*).

DW1 was placed in a holder within a 45% KOH bath at 60°C to conduct a KOH etch (*Figure 2, step 6*). The wafer was periodically removed from the bath and observed with microscopy, and

etch time and channel depth were recorded (see *Table 2*). Channel depth was calculated by finding the change in Z from the upper SiO_2 level to the Si channel base using microscopy. These measurements were used to calculate the etch rates in certain directions (Madou, 2012).

Table 2. Times, resulting Si channel depths, and calculated rates for KOH etching of Si at 45% KOH solution at 60 °C.

Δt in Bath (minutes)	Depth Channel (mm)	Rate (μm /hour)
Extensive*	.03581	-
97	.04812	.1251
120	.06669	.1555
60	.08190	.2534

*Extensive time was used here because it was hypothesized that SiO_2 was still present on the wafer in the intended channel. It was 8 hours of etching.

Pictures were taken of the channel throughout the KOH etch to visually observe its progression (*Figure 6*). Unfortunately, it became evident that some SiO_2 remained on the surface of the wafer and thus the KOH etch took an extended time.

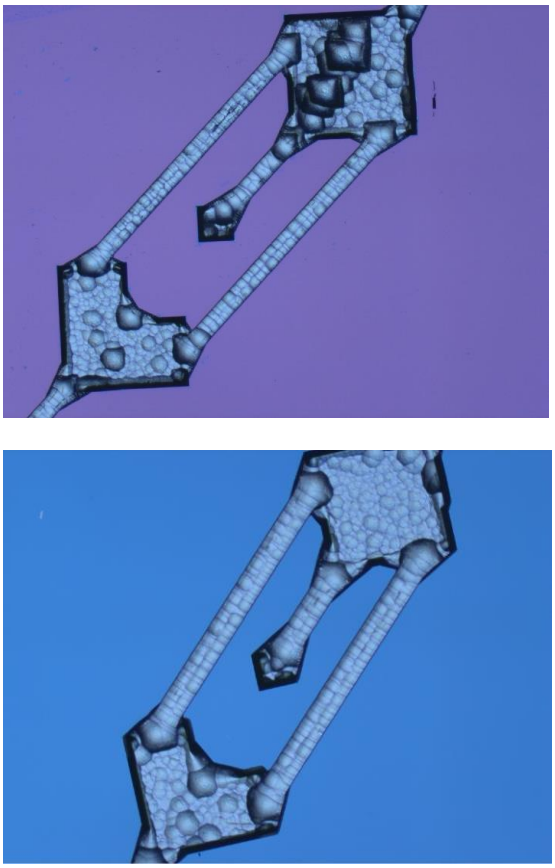

Figure 6. Microscope visualization of nodes on DW1 throughout several stages of the wafer etch.

The wafer was stripped (*Figure 2, step 7*) with buffered oxide etch (BOE), a mixture of NH_4F and HF used for controllable etching of SiO_2, until the SiO_2 was completely absent from the surface (*Figure 7*).

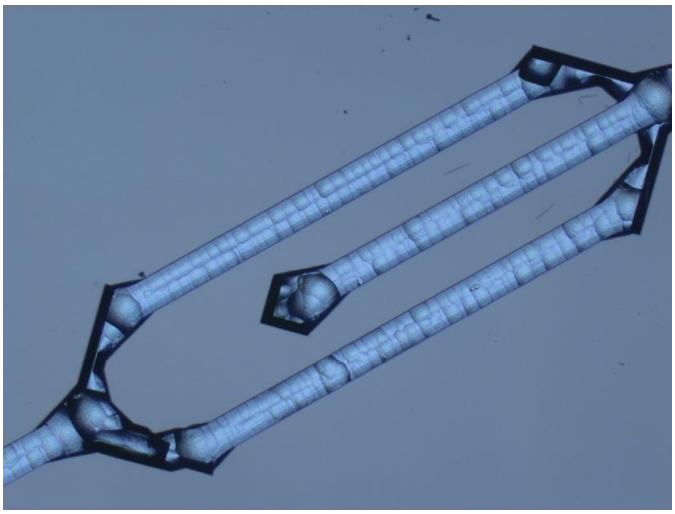

Figure 7. Microscope visualization of a node on DW1 following BOE stripping.

The horizontal widths of the channels were observed before and after stripping using microscope images to determine that there was not a significant underetch (see *Table 3*). An underetch would indicate the channel was etched in a more isotropic manner rather than the desired anisotropic etch, which would theoretically result in relatively straight, flat microchannel walls (*Figure 3, bottom* displays an anisotropic KOH etch).

Table 3. Horizontal channel widths measured on the microscope before and after stripping of silicon dioxide to observe underetching.

Before Stripping (µm)	After Stripping (µm)	Difference (µm)
182.180	186.750	4.570
178.846	173.955	4.891
181.930	186.827	4.897

DW1 had visible defects from the fabrication process and was needed for destructive testing, so it was decided that a new wafer would be created.

Three wafers were prepared for further processing, and the oxidation time was optimized for the thickness required. A second 3 inch Si wafer, SW2, was put into the furnace for oxidation at

1100°C for several cycles to reach roughly 800nm. Finally, two more 3 inch Si wafers, SW3 and SW4, were oxidized for 80 hours (see *Table 4* for all wafer oxidation data).

Table 4. Oxidation times and resulting thicknesses for all wafers.

Wafer	Final Thickness (nm)	Oxidation Times (hours)
DW1	858.04nm	Extensive*, 10, 3, 10
SW1	828.84nm	30, 20, 30
SW2	812.02nm	80
SW3	825.68nm	80

**Extensive time was used because the furnace remained on for an indeterminate period of time.*

DW1 underwent destructive testing through dicing and measurement of etch thicknesses with microscopy. Measurements of the diced DW1 were taken from several angles (see example in *Figure 8*).

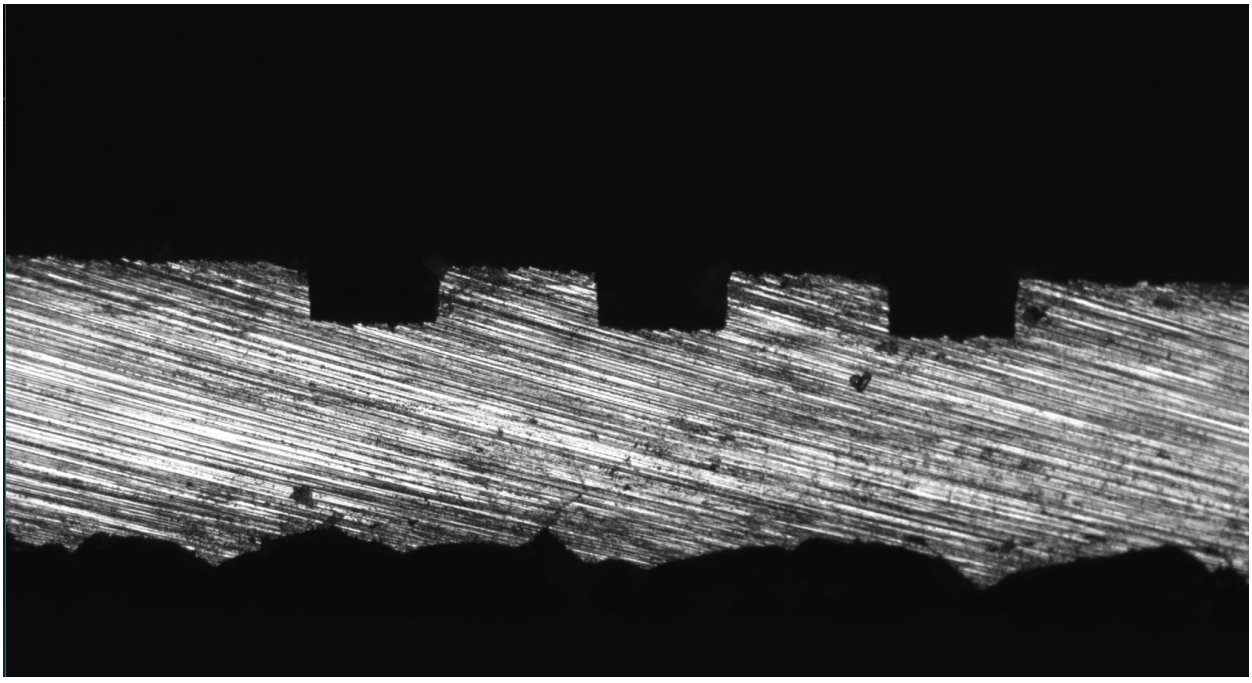

Figure 8. A microscope picture of the diced DW1 from the side. This was used to measure depth and width measurements

This destructive testing demonstrated that the KOH etch rate of Si was roughly a 1:1 ratio at an angle 45° from the wafer flat, as well as into the wafer (see *Table 5*). To fabricate channels of the appropriate width and depth, Mask A had to be altered to account for these etch rates.

Table 5. Microscopy measurements taken on a diced DW1 from the side, in order to measure Si etch rates in different directions under the experimental conditions. Etched width was calculated by taking the width, subtracting 10 µm, and then dividing by two, which accounts for the original mask line width and the etch in two directions on the surface of the wafer.

Depth (µm)	Width (µm)	Etched Width (µm)	Ratio
81.424	182.927	86.4635	1.061892
80.301	179.56	84.78	1.055778
80.38	181.125	85.5625	1.064475

Thus, a new mask, Mask B, was created in AutoCAD (see *Figure 9*) with mask geometries and parameters modified to account for the etch rate relationships. Mask B focused on further characterization of KOH etching in Si for the purpose of fabricating acoustic microchannels with complex geometries. It was also modified to account for a channel width of 100 µm instead of 150 µm as intended in Mask A. Thus elbows, circles, arcs, and nodes with differing geometries were placed aside the modified microchannels. The bifurcation nodes were widened to promote flow (see *Figure 10*).

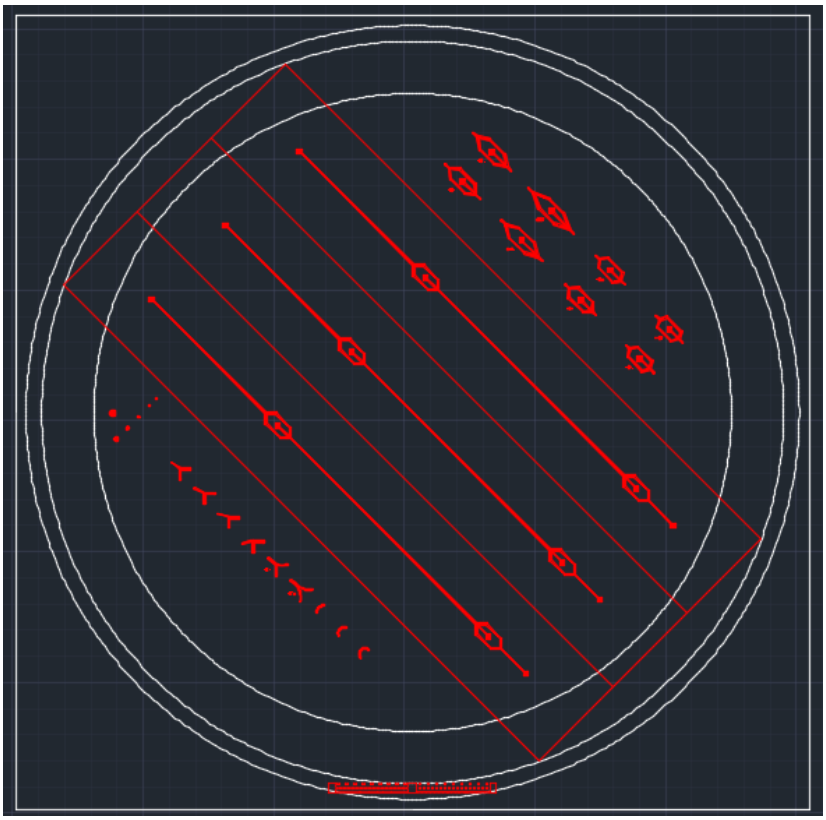

Figure 9. Mask B, two microchannels with a variety of geometries surrounding them for characterization of KOH etching of Si.

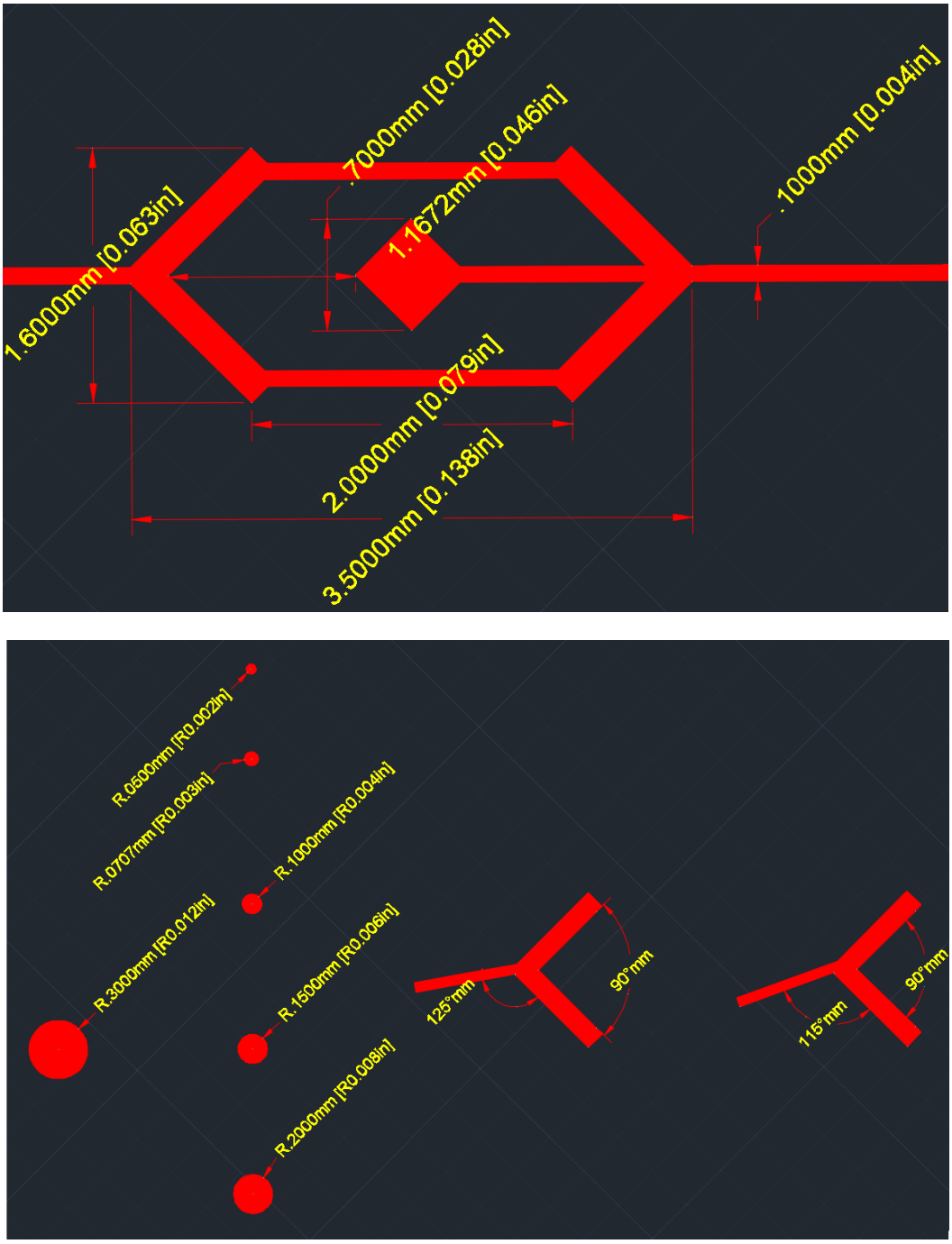

Figure 10. Expanded views of the new bifurcation node (top) and several added features for KOH etch characterization in Si (bottom).

Photolithography was performed on SW3 by the same method as described earlier in this paper, though it was exposed for 21 seconds to account for a change in lamp intensity. Additionally, it was noted that the photoresist changed height significantly with the same spin parameters, at a value of only 24,100 Angstroms, nearly 10,000 Angstroms less than the previous PR thickness, which may result from a change in the viscosity of the 1827 photoresist due to aging. To

replicate this process, spin parameters may need to be retested prior to photolithography to ensure appropriate thickness. RIE was run on SW3 to etch the silicon dioxide, and the parameters for SW3 were significantly different. Overall runtime was 36 minutes, and PR etching as well as difference in the distance between the PR and silicon channel was not found to be consistent or reasonable—this could be due to profilometer calibration issues or an uneven distribution of PR across the wafer. The wafer was etched by RIE until silicon was visible to the naked eye, and following this the wafer was etched with potassium hydroxide as described above. Unlike the previous experiment, the KOH etch was consistent in rate and went for 930 minutes in full. The rate was found to be roughly 9.87 microns/minute, though the rate seemed to spike at the beginning and ending of the etch (see *Figure 11*). The rate of the SiO_2 etch was found to be roughly 0.85 nm/minute, an estimate made using the initial and final thicknesses of the SiO_2 layer.

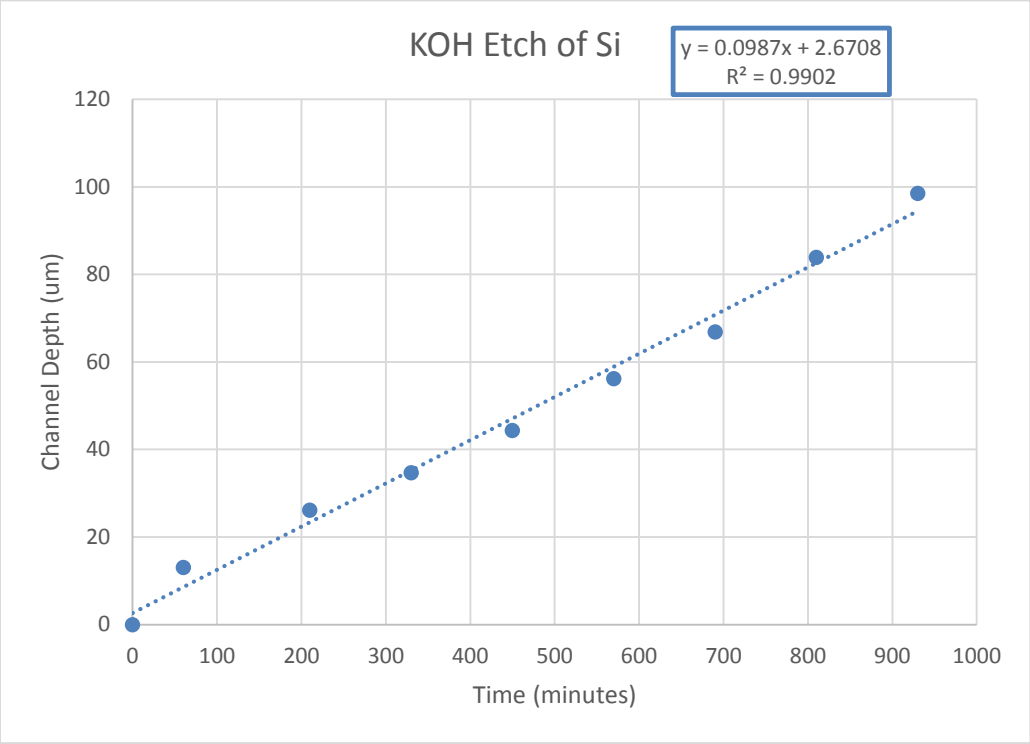

Figure 11. Silicon channel depth measured as a function of time during a potassium hydroxide etch at 60°C with 45% KOH solution.

The channel resulting from the etch appeared smoother than the previous trial with fewer pockmarks; the desired channel depth of roughly 100 microns was achieved.

Future Work:

Future microchannels may be tested for their ability to separate cells in suspension. KOH etching in silicon could be characterized further by studying alternate geometries.

Sources:

Augustsson P, Magnusson C, Nordin M, Lilja H, Laurell T. Anal Chem. 2012;84:7954–7962.

Pal, Prem, and Kazuo Sato. "A Comprehensive Review on Convex and Concave Corners in Silicon Bulk Micromachining Based on Anisotropic Wet Chemical Etching." *Micro and Nano Syst Lett Micro and Nano Systems Letters* 3.1 (2015): n. pag. Web.

Madou, Marc J. *Fundamentals of Microfabrication and Nanotechnology*. Boca Raton, FL: CRC, 2012. Print.

Nilsson, Andreas, Filip Petersson, Henrik Jönsson, and Thomas Laurell. "Acoustic Control of Suspended Particles in Micro Fluidic Chips." *Lab Chip* 4.2 (2004): 131-35. Web.

Thanks To:

Dr. J. Mark Meacham

Michael Binkley

Radoslav Marinov